Journal of Structural Geology 31 (2009) 83–91

Contents lists available at ScienceDirect

Journal of Structural Geology

journal homepage: www.elsevier.com/locate/jsg

An unstable kinematic state of the Himalayan tectonic wedge: Evidence from experimental thrust-spacing patterns

Santanu Bose [a,*], Nibir Mandal [b], Dilip K. Mukhopadhyay [c], Premanand Mishra [c]

[a] Department of Geology, University of Calcutta, 35 Ballygunge Circular Road, Kolkata 700019, West Bengal, India
[b] Indian Institute of Science Education and Research, HC 7 Salt Lake City, Kolkata 700106, India
[c] Department of Earth Sciences, Indian Institute of Technology, Roorkee 247667, Uttaranchal, India

ARTICLE INFO

Article history:
Received 14 March 2008
Received in revised form 30 July 2008
Accepted 9 October 2008
Available online 1 November 2008

Keywords:
Himalayan fold-and-thrust belts
Coulomb rheology
Sandbox experiments
Thrust sequence
Basal friction

ABSTRACT

The frontal tectonic wedge in the NW Himalayas shows a sequence of imbricate thrusts with increasing spacing in the foreland direction. We used analogue model experiments to analyze the thrust pattern in relation to the kinematics of wedge evolution. Experimental findings reveal two kinematic states of the foreland-ward propagation of a wedge: *unstable state and stable state*. The unstable state is characterized by continuous vertical growth of the wedge with progressive horizontal contraction. On the other hand, in the stable state the wedge ceases to grow vertically, but propagates laterally in the foreland direction. In the experimental runs thrust wedges remained in the unstable state even after large horizontal shortening (>50%) when the basal friction was high (∼0.46). Our analysis suggests that successive thrusting occurs always with increasing spacing in unstable wedges, and the rate of increase is larger for larger basal friction. It can maintain uniform spacing only when the wedges turn into the stable state. Using finite element models, we determined the stress distribution in the deforming wedge to find the potential locations of new thrusts in front of a wedge, which also show larger spatial distances with increasing vertical thickness of the wedge. Both physical and numerical models suggest that the tectonic wedge in the NW Himalayan frontal belt has evolved in an unstable state.

1. Introduction

Evolution of fold-and-thrust belts (FTBs) in collisional tectonics has been a focus of study in geodynamics over last several decades (Smoluchowski, 1909; Bucher, 1956; Hubbert and Rubey, 1959; Elliot, 1976; Chapple, 1978; Boyer and Elliot, 1982; Allmendinger, 1992; Dixon and Liu, 1992; Lallemand et al., 1994; Mitra, 1994; Gutscher et al., 1996; Storti et al., 2000; Persson, 2001; Persson and Sokoutis, 2002; Kukowski et al., 2002; Buiter and Schreurs, 2006). FTBs characteristically contain foreland-vergent imbricate thrust systems. The mechanics of thin-skinned accretionary wedges is the most commonly used model to explain sequential development of imbricate thrusts in the wedge. Davis et al. (1983) introduced the concept of critical taper for analyzing the dynamics of Coulomb wedges, leading to instability and shear failure in non-cohesive materials. Later workers have advanced the model considering cohesive materials (Dahlen et al., 1984; Dahlen, 1984; Fletcher, 1989). According to the critically tapered wedge model, an accretionary wedge deforms internally and thereby, increases its taper angle, and at a critical taper the wedge develops internal stresses, leading the system on the verge of failure everywhere. In this dynamic state the basal shear stresses also reach a value required for frictional sliding at the basal detachment (Davis et al., 1983; Boyer and Elliot, 1982; Chapple, 1978). The critically tapered wedge thus tends to slide stably along its base, giving rise to a new thrust in the wedge. It has been shown from physical experiments that the taper angle can fluctuate during sequential thrust progression (Mulugeta and Koyi, 1992). In overall, the critical taper is found to be directly proportional to basal friction (Mulugeta, 1988; Liu et al., 1992; Mandal et al., 1997; Schott and Koyi, 2001). Later studies reveal that there are other geological factors, e.g. fluid activity, which can also influence the critical taper angle (Cobbold and Castro, 1999; Lohrmann et al., 2003; Mourgues and Cobbold, 2006). Several workers have shown that an accretionary prism can develop bi-vergent wedges, depending upon factors like the presence of a singularity at the basal detachment (Willett, 1999; Storti et al., 2000) and the backstop geometry (Persson, 2001; Persson and Sokoutis, 2002). Using physical experiments the growth of bi-vergent wedges has been investigated in great details (Gutscher et al., 1998; Storti et al., 2000; Persson and Sokoutis, 2002).

The critically tapered wedge theory has been extensively used to explain the dynamics favouring the nucleation of a thrust in the wedge. However, it does not give any account for a spatial distribution of thrusts. Field investigations show that thrusts in FTBs are

* Corresponding author. Tel.: +91 9433501266.
E-mail addresses: boses_in@yahoo.com, bose.santanu@gmail.com (S. Bose).

0191-8141/$ – see front matter © 2008 Elsevier Ltd. All rights reserved.
doi:10.1016/j.jsg.2008.10.002

systematically arranged in constituting a foreland-vergent thrust system (Davis et al., 1983; Bally et al., 1966; Price, 1986; Gulick et al., 2004). Different types of rheological models have been employed to enumerate the location of a new thrust in front of a growing accretionary wedge (Bombolakis, 1986; Panian and Pilant, 1990; Goff and Wiltchko, 1992; Schott and Koyi, 2001). These models show that there occurs stress or strain localization at the front of an active thrust along horizontal surfaces, leading to ramping by shear fracturing at a critical stress. The two processes: stress localization and ramping; recur at regular intervals during the foreland-ward propagation of accretionary wedges, giving rise to a sequence of thrusts. There are several factors, such as bed thickness, basal friction, basal slope, surface slope and topographic variations, that determine the spatial distribution of thrusts in the sequences (Bombolakis, 1986; Panian and Pilant, 1990; Mandal et al., 1997; Schott and Koyi, 2001; Mulugeta and Koyi, 1987). Mandal et al. (1997) have shown that thrust spacing is a linear function of bed thickness for wedges with negligible surface slopes, and the relation turns into non-linear when the surface slope becomes significant. These studies also reveal that thrust spacing is inversely related to basal friction. In physical experiments consecutive thrusts develop with varying spacing (Liu et al., 1992; Mandal et al., 1997; Lujan et al., 2003). However, there has not been any thorough analysis of such spatial variations in relation to different physical parameters, and we still need to understand the spatial arrangements of thrusts in the context of the mechanics of wedge growth.

We studied thrust sequences in the Nahan thrust belt located in the frontal part of the NW Himalaya (Fig. 1). The sequences show systematically arranged foreland-vergent thrusts, and their balanced cross-sections reveal marked variations of thrust spacing in the foreland direction. Using analogue experiments this paper presents a quantitative analysis of thrust-spacing variation as

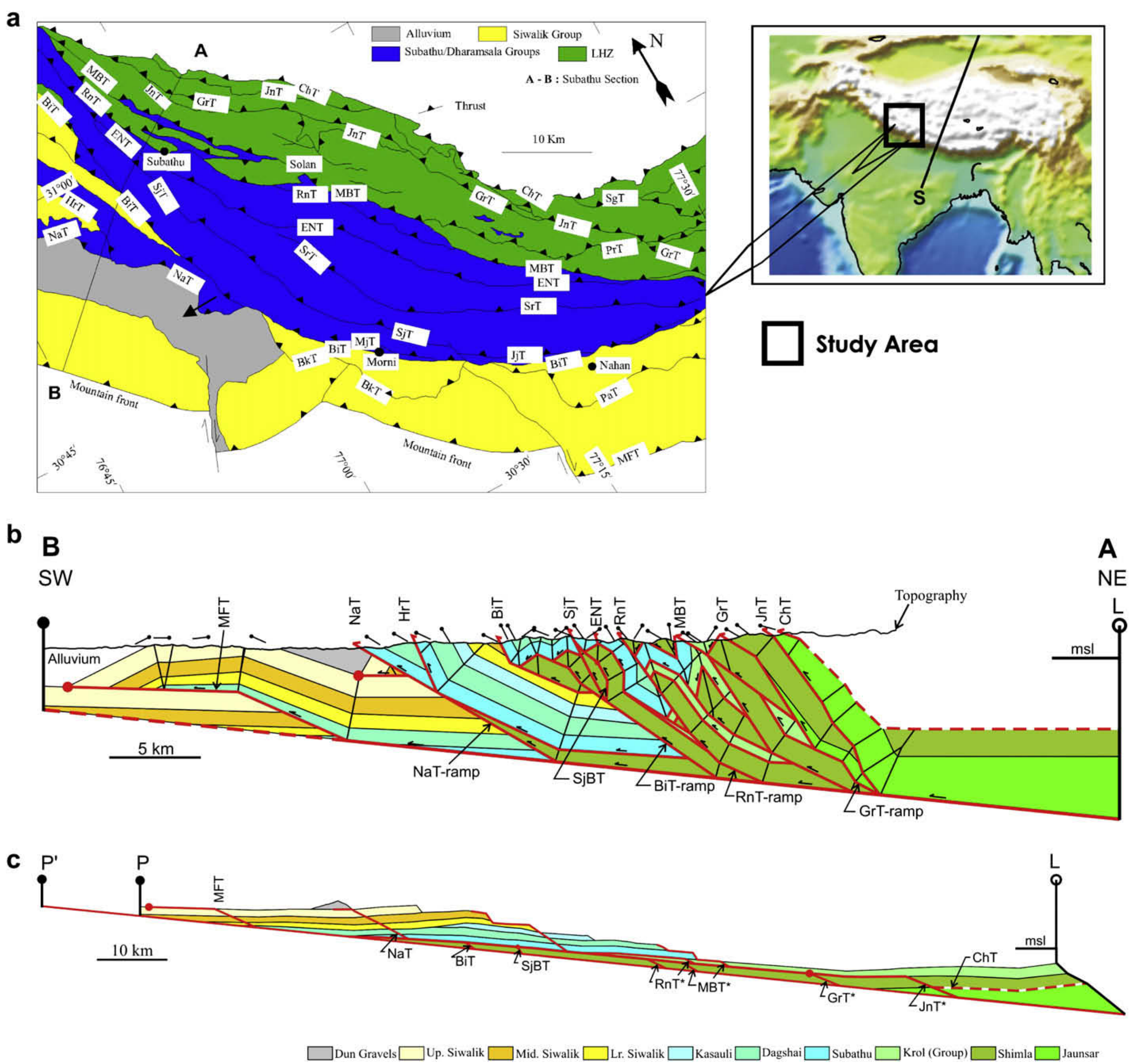

Fig. 1. (a) Structural map of hinterland-dipping imbricate thrusts (local names indicated) in the Nahan Salient, NW Himalaya. (b) Thrust architecture on Subathu section [AB line in (a)]. (c) A restored section of a part of the thrust sequence shown in (b). Note that the thrust spacing increases discernibly in the foreland direction.

a function of the kinematics of wedge growth. We performed a series of sandbox experiments to develop thrust wedges, and estimated the lateral spacing of successively formed frontal thrusts in the course of wedge growth. The experimental findings finally explain the kinematic conditions of wedge growth and the basal friction, resulting in variation of thrust spacing observed in the Himalayan thrust belt. The analysis is complemented with results obtained from finite element modelling of stress distribution in a deforming wedge.

2. Thrust wedge in the Subathu section, NW Himalayas

In this section we briefly describe the thrust architecture in the frontal part of the Himalayan orogenic belt, which shows all the characters of a typical fold-and-thrust belt (FTB) (Mukhopadhyay and Mishra, 2005, 1999; Thakur, 1993). The Nahan Salient in the NW Himalayan FTB contains Tertiary sedimentary rock sequences with gentle arcuate map pattern (Fig. 1a). A number of longitudinally continuous thrusts with dips approximately in the NE direction are present in this area. Absence of back thrusts in this wedge suggests that the thrust sequence have evolved probably with a high-basal friction (Liu et al., 1992; Mandal et al., 1997).

The NW Himalayan FTB shows a series of thrusts with varying spatial arrangements (Fig. 1a). In the Subathu section of this belt thrust splays show a complex geometrical distribution in the hinterland (Fig. 1b). We carefully considered thrust splays, branching from the same basal detachment, and studied qualitatively their spatial arrangement from the hinterland to foreland. In overall, the thrust spacing increases monotonically in the foreland direction. Thrusts in the hinterland are closely spaced showing an average spacing of about 2 km, which increases to 4.5 km in the middle part, and to 7.5 km in the extreme frontal part of the mountain. Such an increase in spacing is also evident in the tectonic profiles and restored cross-sections (Fig. 1b and c). In order to investigate this spatial variation of thrusts, sets of analogue experiments were run by varying basal friction. We present the experiments and their results in the following section.

3. Analogue model experiments

3.1. Approach

We used non-cohesive natural sand (Coulomb material) in analogue model experiments (Davis et al., 1983; Hubbert, 1951). Loose sand appears to be a suitable material for scaled model experiments simulating large-scale brittle deformations in the uppermost crust (Davis et al., 1983; Mulugeta, 1988; Liu et al., 1992; Mandal et al., 1997). The method of model preparation was similar to that employed in earlier studies (Davis et al., 1983; Mulugeta, 1988; Liu et al., 1992; Mandal et al., 1997; Lujan et al., 2003; Koyi, 1995; Yamada et al., 2006). The experimental apparatus consists of a 100 cm long and 25 cm wide glass-sided box. Well-sorted aeolian quartz sand with an average grain size of 500 μm, with bulk density $\rho = 1.6\ \mathrm{gm/cm^3}$ and internal co-efficient of friction, $\mu = 0.57$, were sieved on the base of the sandbox to build layered sand beds by sieving alternately white sand and red colored sand. All the beds had uniform initial thickness ($\sim$1.5 cm).

A series of experiments were carried out by resting sand models over a rigid base with different basal friction (μ_b). We sprinkled boric powder over the rigid glass base to obtain low basal friction ($\mu_b = 0.36$). For high-basal friction ($\mu_b = 0.46$) a coarse (30 mesh) sandpaper was glued to the base. The moderate basal friction ($\mu_b = 0.41$) was obtained by sieving a veneer of talc at the interface of sand bed and base. The four side glasses of the sandbox were cleaned and dried carefully by heating to remove surface moisture. Such a treatment was required to avoid sticking of sand to the glass sidewalls.

The model was deformed in a pure shear box by moving a screw driven buttress from one side in the horizontal direction at a constant velocity of 0.3 mm/s. The geometry of wedge developed in sand beds depends on the shape of the buttress (Byrne et al., 1988; Koons, 1990; Calassou et al., 1993; Persson and Sokoutis, 2002). We used a planar, vertical buttress in our experimental set-up in order to simulate mono-vergent wedges (cf. Mulugeta, 1988; Mulugeta and Koyi, 1992; Liu et al., 1992; Storti and McClay, 1995; Mandal et al., 1997). During an experimental run photographs of progressively developing thrusts in the models were captured, keeping the camera at a fixed distance from the model. The thrust spacing was measured from successive photographs snapped at the instant of initiation of new thrusts.

3.2. Analysis of thrust spacing in wedges

The experimental runs reveal that a critically tapered wedge can be either in a *stable* or an *unstable* state (Fig. 2). In the unstable state the wedges continue to grow vertically during their frontal propagation (Fig. 2a), whereas they cease to grow vertically on attaining the stable state, and accommodate the horizontal shortening entirely by foreland-ward propagation (Fig. 2b). The two states are phenomenologically similar to the sequential stages (Stage I and Stage II) of bi-vergent wedges described by Storti et al. (2000). Stages I and II are characterized by retro-wedge and pro-wedge thrusting, respectively. In our study we, however, define the two states for describing the growth kinematics of mono-vergent wedges propagating in the foreland direction. We discuss below how the kinematic state can influence the progressive development of foreland-vergent thrusts.

For low basal friction ($\mu_b = 0.36$), successive thrusts formed with wide spacing, and the vertical growth of wedges involved relatively smaller displacements along individual thrusts. The wedge had a taper of about 9°–10° (Fig. 3a). In the condition of low basal friction, the thrust spacing increased, but had a tendency to attain a stationary value at a low bulk shortening (<30%) (Fig. 4a). The kinematic evolution of thrust wedges can be analyzed by considering parameters, such as wedge height and the ratio of shortening and wedge height (Storti and McClay, 1995). We studied the variation of wedge height as a function of the horizontal shortening. The wedge attained a stable state for a small bulk shortening ($\sim$30%), and then propagated in the foreland direction maintaining

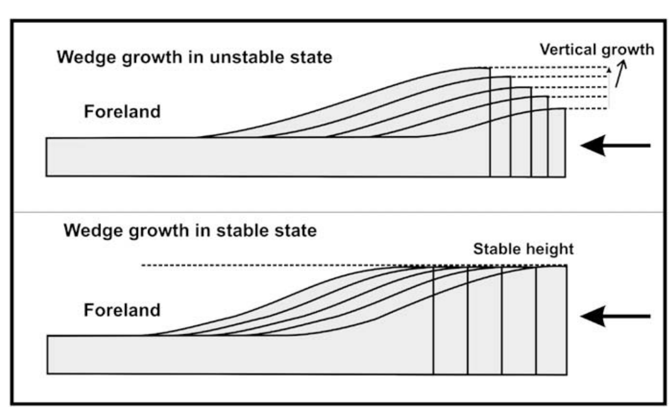

Fig. 2. Two principal kinematic states of accretionary wedges. (a) *Unstable state*: the wedge grows vertically, and its maximum height increases continuously with progressive horizontal contraction. (b) *Stable state*: the wedge propagates in the foreland direction maintaining a constant vertical height. Horizontal arrows show shortening from right to left. Dashed lines indicate instantaneous maximum heights of the wedges.

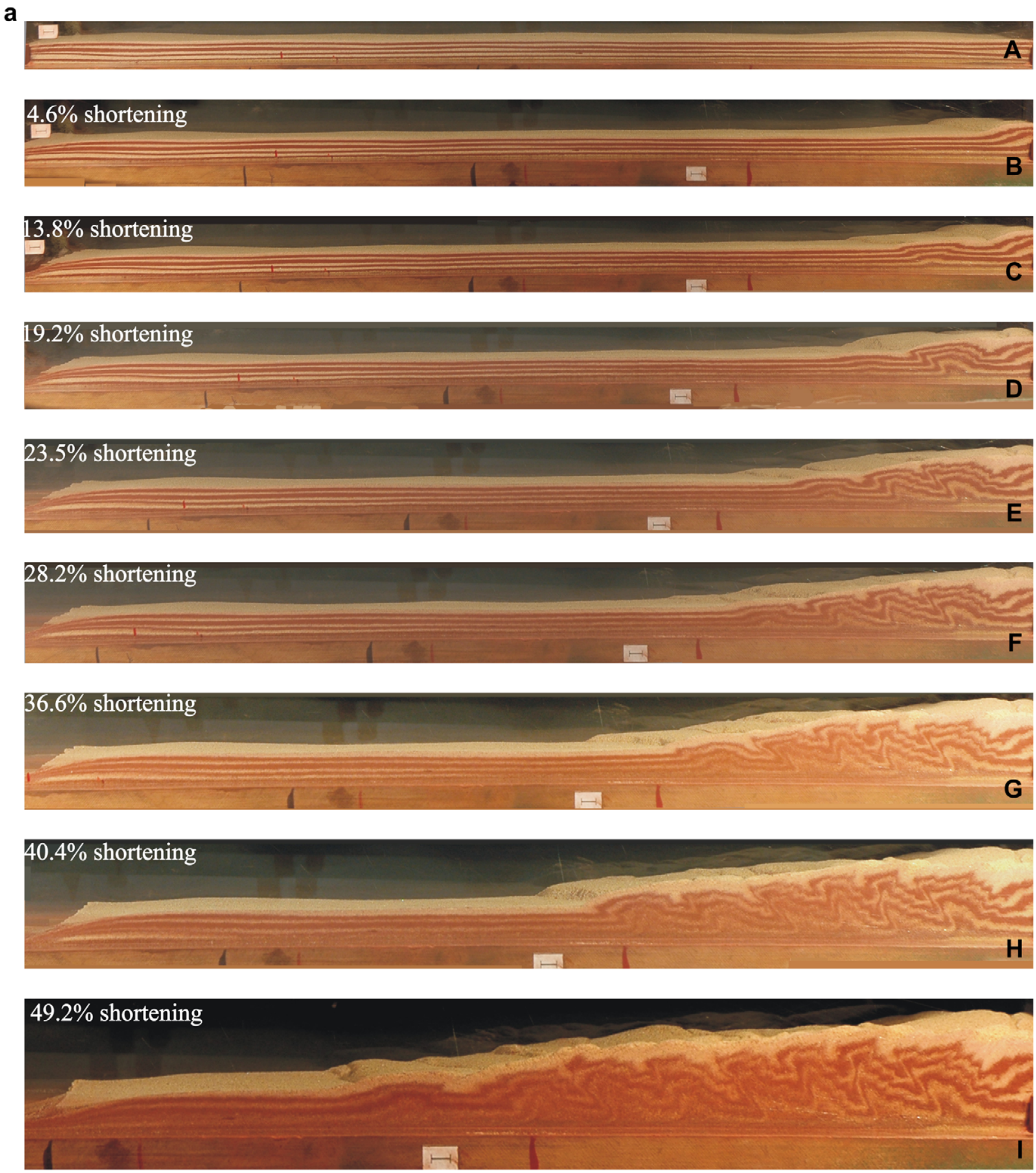

Fig. 3. Progressive development of imbricate thrust systems in sand models with (a) low ($\mu_b = 0.36$), (b) moderate ($\mu_b = 0.\ 41$) and (c) high ($\mu_b = 0.46$) basal friction. Note that frontal thrusts in (c) show a strong variation in their spacing. Models were deformed by horizontal contraction (right to left). Scale bar: 1 cm.

that stable height (Fig. 4b). Further horizontal shortening was accommodated entirely by lateral propagation of the wedge, giving rise to a plateau-like topography in the hinterland. We tested the stability behaviour of the wedge in progressive deformations. It was observed that the stable height remained persistent even when the experimental run was continued with a large amount of shortening (>50%) (Fig. 4b). In some experiments, however, there were small fluctuations of elevation in the stable state, which might have occurred due to reactivation of older thrusts in the hinterland. Albeit, the wedge immediately regained its stability as such thrusts became inactive in the course of progressive shortening.

In experiments with high-basal friction ($\mu_b = 0.46$) wedges had relatively larger taper angles (~19°; Fig. 3c), as also observed in earlier experiments (Liu et al., 1992). The wedges continued to grow vertically with increasing shortening and remained in the unstable state even when the bulk finite horizontal shortening was large (>50%) (Fig. 4b). The contrasting growth history in models with high and low basal frictions is reflected in the spatial distribution of

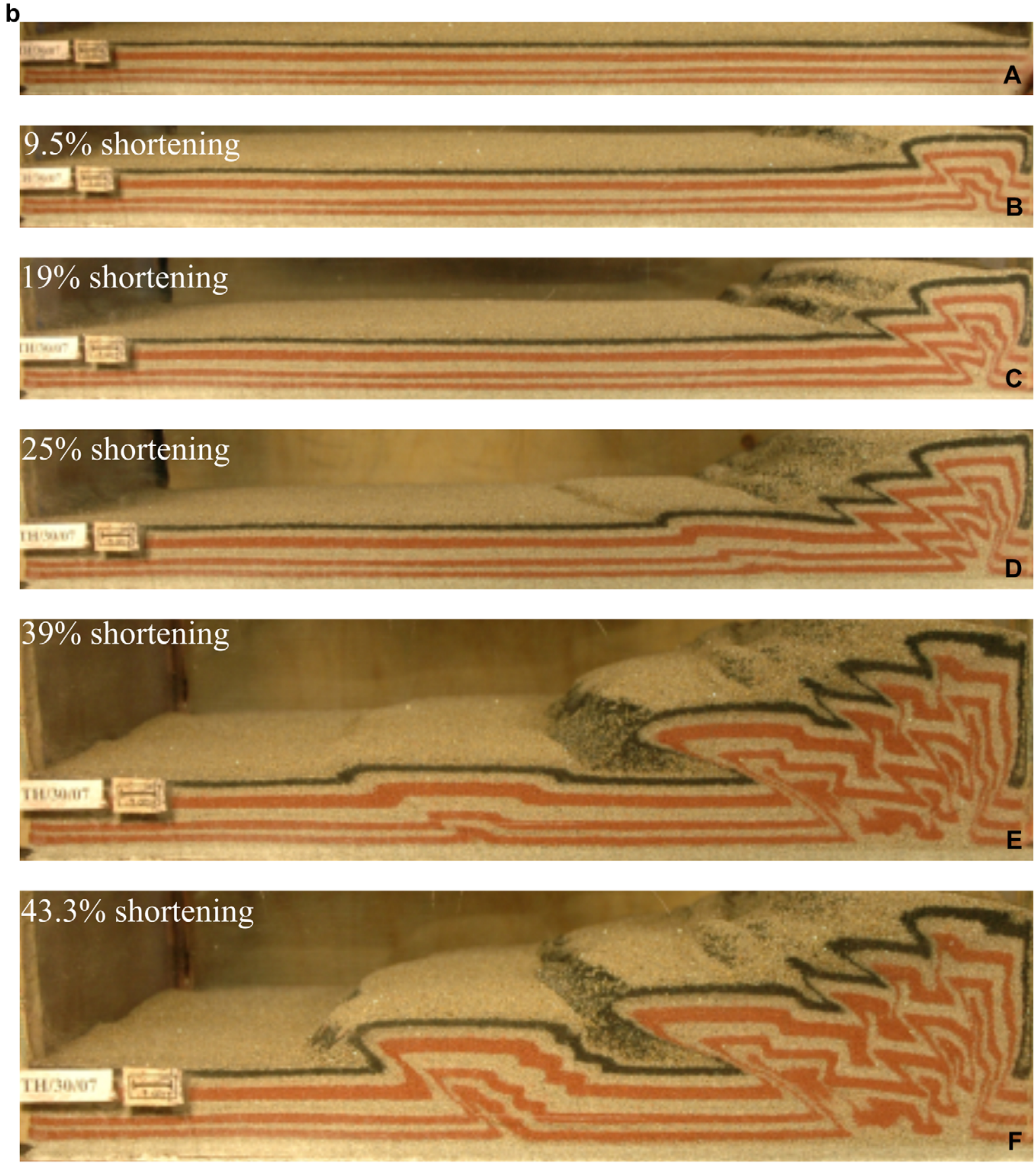

Fig. 3. (*continued*).

successive imbricate thrusts. The thrust spacing continues to increase and does not assume a stationary value if the basal friction is high (Fig. 4a). Moreover, there was a large displacement on a thrust prior to initiation of a new imbricate thrust in the footwall. This may lead to back rotation of earlier thrusts in the hangingwall of an evolving thrust, as noted by Mukhopadhyay and Mishra (2005). The spatial arrangement of frontal thrusts in the deformed sand models with high-basal friction is qualitatively similar to that noticed in the Subathu section of the NW Himalayan wedge (Fig. 1b).

For moderate basal friction ($\mu_b = 0.41$), the style of wedge growth was intermediate between those for high and low basal friction described above, and the wedges had an average taper angle of 13° (Fig. 3b). Fig. 4a shows the development of successive thrusts with increasing spacing during wedge growth. However, the spacing approaches a stationary value asymptotically when the finite bulk shortening in the model was around 41%.

The principal experimental findings are outlined along following points. (1) The kinematic evolution of a thrust wedge

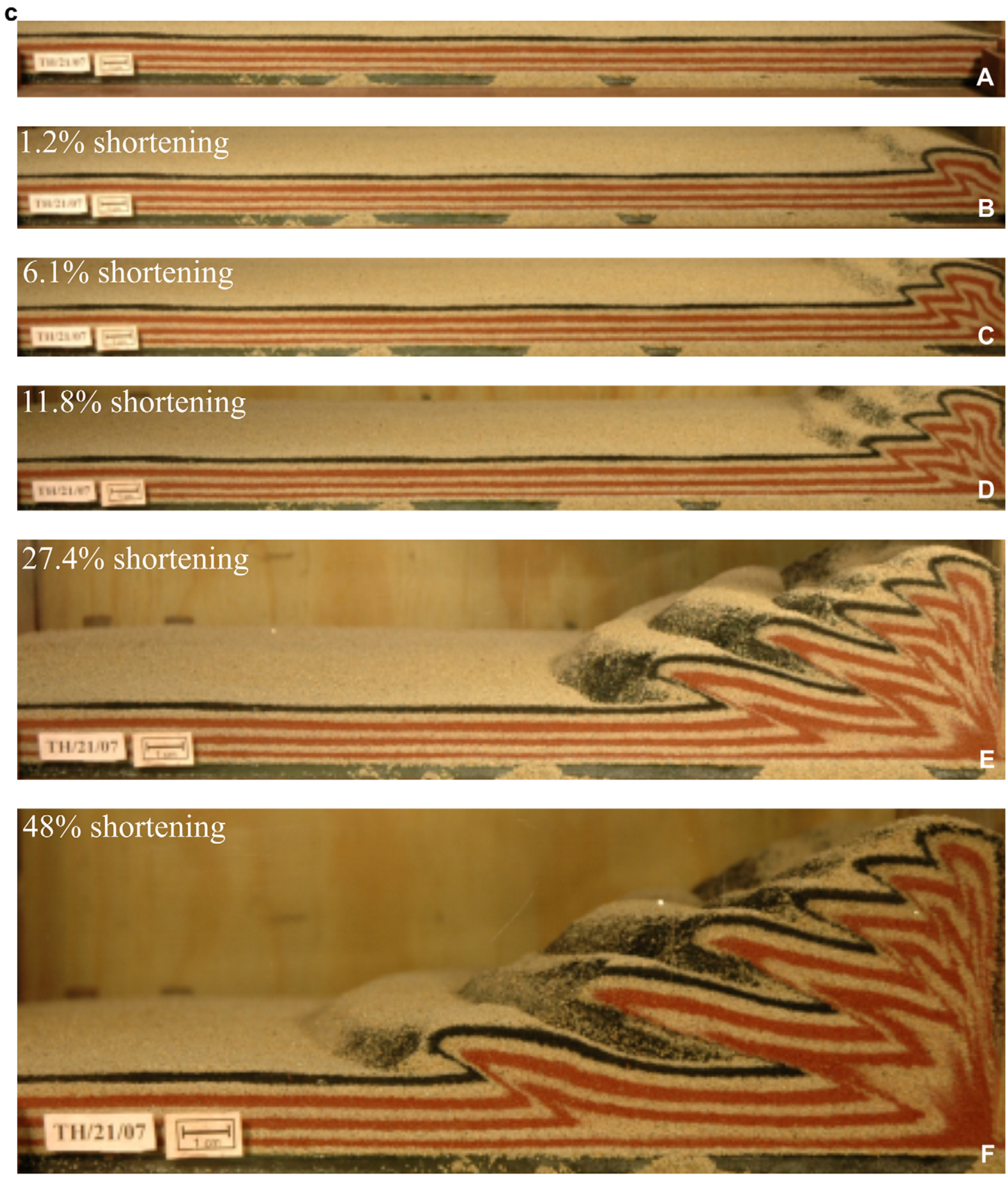

Fig. 3. (*continued*).

takes place in two states: unstable (*continued vertical growth*) and stable (*cessation of vertical growth*) states. (2) In the unstable state imbricate thrusts form sequentially with increasing horizontal spacing, and the variation tends to die out as the wedge attains the stable state. (3) With increasing basal friction the wedges remain in the unstable state for large amount of horizontal tectonic contraction, and show imbricate thrusts with strongly varying spacing.

4. Finite element modelling

We employed finite element models to investigate the stress distribution as a function of wedge geometry, and explain varying thrust spacing in the Subathu section and model experiments (Figs. 1b and 3c). In this analysis the von-Mises stresses (σ_v) were considered for determining the potential zones of shear failure (Jaeger, 1969). This stress was calculated using the following equation.

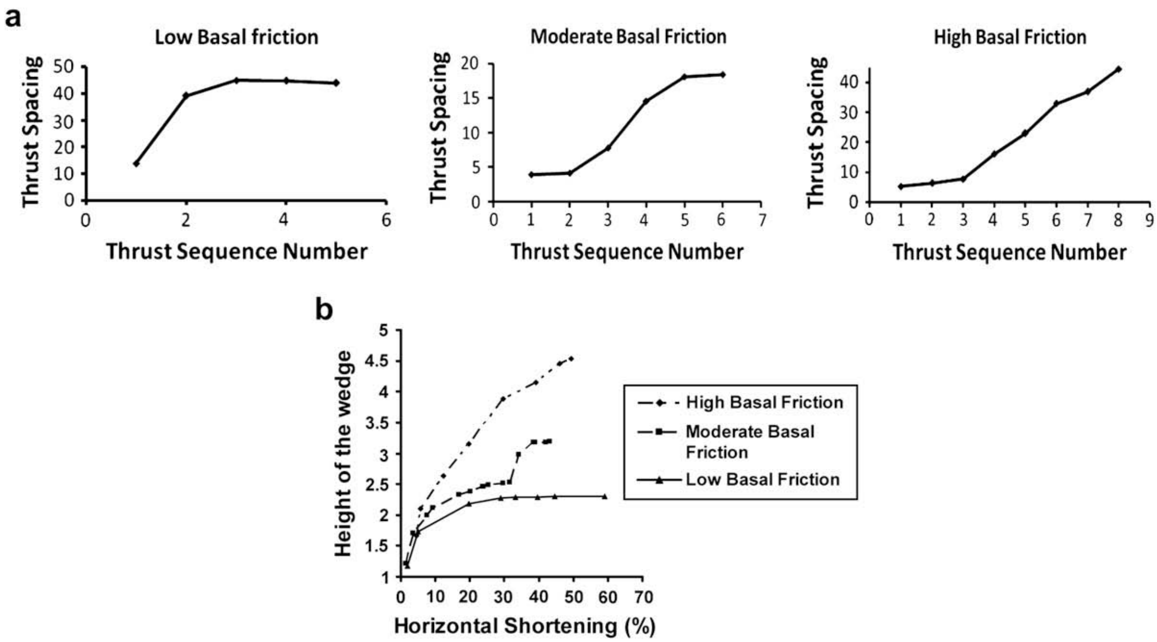

Fig. 4. (a) Three graphs (left to right) present the variations in spacing (in mm) between two consecutive thrusts formed in the course of wedge growth for low, moderate and high-basal friction. Initial thickness of beds in the three cases was held constant. (b) Variation of wedge height (in cm) with finite bulk horizontal shortening in the models.

$$\sigma_v = \sqrt{(\sigma_1 - \sigma_2)^2 + (\sigma_2 - \sigma_3)^2 + (\sigma_1 - \sigma_3)^2} \quad (1)$$

where σ_1, σ_2, and σ_1 are the principal stresses. It may be noted that a body first undergoes shear failure along zones of maximum von-Mises stress (σ_v) in Eq. (1).

The model was developed by taking a visco-elastic layer on a horizontal base with frictional contact. The co-efficient of friction was 0.5 representing the analogue experimental model with high-basal friction. The constitutive rheological equation follows:

$$\frac{d\varepsilon}{dt} = \frac{1}{2\mu}\frac{d\sigma}{dt} + \frac{\sigma}{2\eta}, \quad (2)$$

where ε and σ are instantaneous strain and stress in the medium, respectively (Turcotte and Schubert, 2002). In the finite element modelling, the co-efficient of viscosity and shear modulus were chosen in the order of 10^{21} Pa s and 10^{10} Pa, respectively. Initial models were designed with wedge shapes of varying vertical thicknesses at the hinterland. The prime aim of this modelling experiment was to determine the influence of the initial vertical

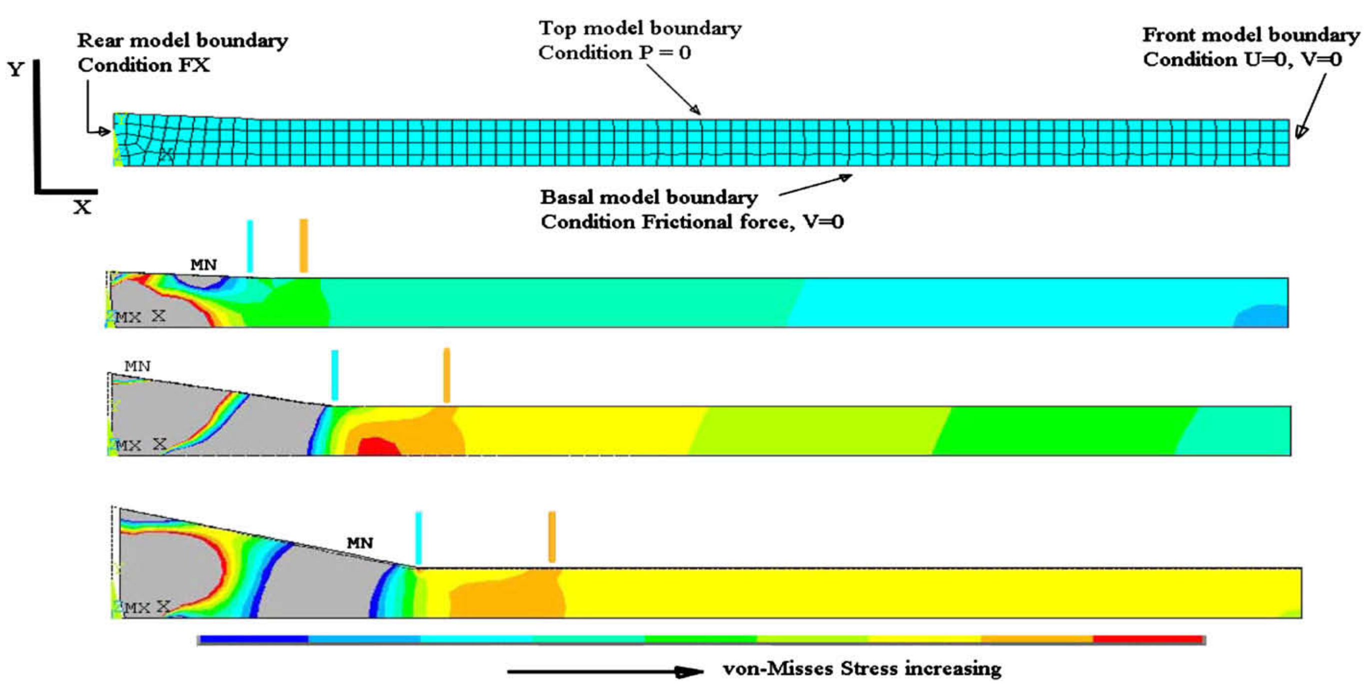

Fig. 5. Stress analysis of wedges simulated in finite element models. Color shades indicate the magnitude of von-Mises stresses. Note that localization of high von-Mises stresses in front of the wedges, revealing the potential locations of new thrusts. Also, notice that the distance of new thrust (brown vertical bar) from the front (blue bar) is larger for larger vertical height of wedges.

thickness on the location of the maximum von-Mises stress that may indicate position of thrust initiation (shear failure) from the wedge front.

The models were deformed with the following boundary conditions (Fig. 5).

(1) Top model boundary: unconstrained condition and pressure $(p) = 0$.
(2) Basal model boundary: $v = 0$ and frictional force, $F_x = \rho g h$, where v is the vertical velocity component, and ρ, g and h are density of the medium, acceleration due to gravity and sectional thickness, respectively.
(3) Rear model boundary: $u = U$ and v is unconstrained. u is the horizontal velocity component.
(4) Frontal model boundary: $u = 0$ and $v = 0$.

We mapped the von-Mises stress in the deformed wedges, the maximum of which were observed to localize along an inclined zone in front of the wedge (Fig. 5). This zone is evidently the location of new thrust at that instant. Models of increasing vertical thickness show increasing distance of this inclined zone from the wedge front. The model results thus confirmed the experimental findings that successive new thrusts will grow with increasing spacing in the vertically growing (unstable state) wedges.

5. Discussions

The structural geometry in the frontal tectonic wedge of the NW Himalaya shows a spatial variation from the foreland to hinterland. This variation is mostly a manifestation of variation in thrust spacing. Towards foreland larger thrust spacing leads to simple structural geometry with widely spaced ramp anticlines. Thrust spacing decreases in the hinterland direction with accompanying complexity in structural geometry. We discuss below the implications of our experimental findings in the light of kinematic behaviour of tectonic wedges.

The experiments presented in Section 3 suggest that the internal architecture of thrusts constituting a wedge seems to be sensitive to the critical taper, which is a function of basal friction. Wedges with low basal friction attained a low critical taper, where successively formed thrusts had a tendency to achieve uniform spacing at an early stage of horizontal shortening. On the other hand, those with higher basal friction had a large taper, and developed successive thrusts with continuously increasing spacing. It thus appears that basal friction also controls the spatial variation of frontal thrust progression. Several workers have used thrust spacing for estimating the basal friction in fold-and-thrust belts (Mandal et al., 1997; Schott and Koyi, 2001). Based on the experimental observations, we propose that the gradient in variation of spacing in imbricate thrust systems can be considered as an additional parameter for analyzing, at least qualitatively the nature of basal friction prevailing in the tectonic wedge.

We studied the progressive growth of a wedge in an experimental run, which reveals that the maximum height of wedge continuously increases with successive thrusting. However, the wedge attained a stage when the height did not increase even though the process of thrusting continued to occur with further horizontal bulk shortening. The wedge thereby grew laterally, maintaining a constant height at the hinterland, which we have described as *stable state* growth of wedge. Attainment of the *stable state* of the wedge requires a significant amount of bulk finite shortening in the thrust system, as revealed from the experiments presented in this paper (Fig. 4b). The amount of critical shortening depends on the basal friction. For example, the bulk shortening required for developing a stable wedge in experiment was 32% when the basal friction was 0.36. On the other hand, it was 41% for basal friction of 0.41. In the experimental run, the wedge did not attain a stable state even after more than 50% bulk shortening in case of extremely high-basal friction (0.5). It thus follows that the wedge growth in an *unstable state* occupies a significant part of the evolutionary history of fold-and-thrust belts, and must be taken into account in order to interpret the spatial arrangement of frontal thrusts in imbricate thrust systems. Experiments with low and moderate basal friction show that successive frontal thrusts in the unstable state develop with increasing spacing, which tends to be steady when the wedge switches from unstable to stable state (Fig. 4a). Thrusts in wedges with high-basal friction continue to increase their spacing, as the wedges remained unstable during the experimental runs (Fig. 3c). Thrust-spacing distributions can thus be used for recognizing the mechanical state of a thrust wedge. For example, increasing thrust spacing in the Subathu section suggests that the NW Himalayan frontal wedge has developed in the *unstable state*.

In our experiments we did not consider the effects of erosion at the surface of thrust wedges. However, most of the convergent tectonic belts involve syn-orogenic erosional processes. Several workers have shown that the rate of erosion is a crucial factor in controlling the dynamics of orogenic wedges (Dahlen and Suppe, 1988; Beaumont et al., 1992, 2001; Willett and Beaumont, 1994; Willett, 1999; Hilley and Strecker, 2004). The erosion factor will also play a role in determining the stability of wedges. Intuitively, a wedge is not likely to attain a stable state if syn-orogenic erosion takes place at high rates resulting in denudation of the elevated regions of the fold-and-thrust belts. In such a situation, successive imbricate thrusts will show a variable spatial distribution.

6. Conclusions

The principal outcomes of this study are concluded below:

(1) Evolution of mono-vergent thrust wedges can be described in terms of two states: *unstable* and *stable*. In the unstable state, a wedge grows vertically, and increases the hinterland elevation during its foreland-ward propagation. On the other hand, the hinterland elevation ceases to occur in the stable state, and the wedge propagates laterally in the foreland direction by maintaining a constant hinterland elevation. The transition between an unstable and a stable state can occur sequentially in progressive convergence movements.
(2) Basal friction determines the kinematic state of growing wedges. In case of low basal friction, a wedge attains a stable state immediately with progressive horizontal shortening ($<$30%), whereas that growing in high-basal condition remains in the unstable even after large horizontal shortening ($>$50%)
(3) Frontal thrusts develop essentially with increasing lateral spacing when the wedge is in the unstable state. In contrast, they develop maintaining a constant spacing if the wedge occurs in the stable state.
(4) Varying thrust spacing in the Nahan belt indicates an unstable kinematic state in the frontal part of the NW Himalaya.

Acknowledgements

We are grateful to Profs. P. Cobbold and F. Storti for their insightful reviews and many constructive suggestions for improvement of the manuscript and Prof. J. Hippertt for giving us an outline for revising the manuscript. We thank Prof. Chandan Chakraborty for constructive discussions in the course of this study. The present work was supported by the Department of Science and Technology, India. UGC, India is also acknowledged for the infrastructural facilities.

References

Allmendinger, R.W., 1992. Fold and thrust tectonics of the western United States exclusive of the accreted terranes. In: Burchfiel, B.C., Lipman, P.W., Zoback, M.L. (Eds.), The Cordilleran Orogen, The Conterminous U.S.. The Geology of North America, vol. G-3 Geological Society of America, pp. 583–608.

Bally, A.W., Gordy, P.L., Stewart, G.A., 1966. Structure, seismic data and orogenic evolution of southern Canadian Rocky Mountains. Can. J. Pet. Geol. 14, 337–381.

Beaumont, C., Fullsack, P., Hamilton, J., 1992. Erosional control of active compressional orogens. In: McClay, K.R. (Ed.), Thrust Tectonics. Chapman and Hall, London, pp. 1–18.

Beaumont, C., Jamieson, R.A., Nguyen, M.H., Lee, B., 2001. Himalayan tectonics explained by extrusion of a low-viscosity crustal channel coupled to focused surface denudation. Nature 414, 738–742.

Bombolakis, E.G., 1986. Thrust-fault mechanics and origin of a frontal ramp. J. Struct. Geol. 8, 281–290.

Boyer, S.E., Elliot, D., 1982. Thrust systems. Am. Assoc. Pet. Geol. Bull., 1196–1230.

Bucher, W.H., 1956. The role of gravity in orogenisis. Geol. Soc. Am. Bull. 67, 1295–1318.

Buiter, S.J.H., Schreurs, G. (Eds.), 2006. Analogue and Numerical Modeling of Crustal-Scale Processes. Geological Society London, Special Publications, p. 253.

Byrne, D.E., Davis, D.M., Lynn, R.S., 1988. Loci and maximum size of thrust earthquakes and the mechanics of the shallow region of subduction zones. Tectonics 7, 833–857.

Calassou, S., Larroque, C., Malavieille, J., 1993. Transfer zones of deformation in thrust wedges: an experimental study. Tectonophysics 221, 325–344.

Chapple, W.M., 1978. Mechanics of thin-skinned fold-and-thrust belts. Geol. Soc. Am. Bull. 89, 1189–1198.

Cobbold, P.R., Castro, L., 1999. Fluid pressure and effective stress in sandbox models. Tectonophysics 301 (1), 1–19.

Dahlen, F.A., Suppe, J., Davis, D.M., 1984. Mechanics of fold-and-thrust belts and accretionary wedges: cohesive coulomb theory. J. Geophys. Res. 89, 10087–10101.

Dahlen, F.A., 1984. Noncohesive critical coulomb wedges: an exact solution. J. Geophys. Res. 89, 10125–10133.

Dahlen, F.A., Suppe, J., 1988. Mechanics, growth and erosion of mountain belts. Geol. Soc. Am. Special Paper 218, 161–178.

Davis, D.M., Suppe, J., Dahlen, F.A., 1983. Mechanics of fold-and-thrust belts and accretionary wedges. J. Geophys. Res. 88, 1153–1172.

Dixon, J.M., Liu, S., 1992. Centrifuge modeling of the propagation of thrust faults. In: McClay, K.R. (Ed.), Thrust Tectonics. Chapman and Hall, London, pp. 53–69.

Elliot, D., 1976. The motion of thrust sheets. J. Geophys. Res. 81, 949–963.

Fletcher, R.C., 1989. Approximate analytical solutions for a cohesive fold-and-thrust wedge: some results for lateral variation in wedge properties and for finite wedge angle. J. Geophys. Res. 94, 10347–10354.

Goff, D., Wiltchko, D.V., 1992. Stresses beneath a ramping thrust sheet. J. Struct. Geol. 14, 437–449.

Gulick, S.P.S., Bangs, N.L.B., Shipley, T.H., Nakamura, Y., Moore, G., Kuramoto, S., 2004. Three-dimensional architecture of the Nankai accretionary prism's imbricate thrust zone off Cape Muroto, Japan: prism reconstruction via en echelon thrust propagation. J. Geophys. Res. 109, B02105, doi:10.1029/2003JB002654.

Gutscher, M.A., Kukowski, N., Malavieille, J., Lallemand, S., 1996. Cyclical behavior of thrust wedges; insights from high basal friction sandbox experiments. Geology 24, 135–138.

Gutscher, M.A., Kukowski, N., Malavieille, J., Lallemand, S., 1998. Material transfer in accretionary wedges from analysis of a systematic series of analog experiments. J. Struct. Geol. 20, 407–416.

Hilley, G.E., Strecker, M.R., 2004. Steady state erosion of critical Coulomb wedges with applications to Taiwan and the Himalaya. J. Geophys. Res. 109, 1–17.

Hubbert, M.K., 1951. Mechanical basis for certain familiar geologic structures. Geol. Soc. Am. Bull. 62, 355–372.

Hubbert, M.K., Rubey, W.W., 1959. Role of fluid pressure in the mechanics of overthrust faulting. I. Mechanics of fluid-filled porous solid and its application to overthrust faulting. Bull. Geol. Soc. Am. 70, 115–166.

Jaeger, J.C., 1969. Elasticity, Fracture and Flow with Engineering and Geological Applications. Methuen & Co Ltd., p 268.

Koons, P.O., 1990. The two-sided orogen: collision and erosion from the sandbox to the Southern Alps, New Zealand. Geology 18, 679–682.

Koyi, H., 1995. Mode of internal deformation of sand wedges. J. Struct. Geol. 17, 293–300.

Kukowski, N., Lallemand, S.E., Malavieille, J., Gutscher, M.A., Reston, T.J., 2002. Mechanical decoupling and basal duplex formation observed in sandbox experiments with application to the Western Mediterranean Ridge accretionary complex. Mar. Geol. 3068, 1–13.

Lallemand, S.E., Schnuerle, P., Malavieille, J., 1994. Coulomb theory applied to accretionary and nonaccretionary wedges; possible causes for tectonic erosion and/or frontal accretion. J. Geophys. Res. Solid Earth Planet. 99, 12033–12055.

Liu, H., McClay, K.R., Powell, D., 1992. Physical models of thrust wedges. In: McClay, K.R. (Ed.), Thrust Tectonics. Chapman and Hall, London, pp. 71–81.

Lohrmann, J., Kokowski, N., Adam, J., Oncken, O., 2003. The impact of analogue materials properties on the geometry, kinematics, and dynamics of convergent sand wedges. J. Struct. Geol. 25, 1691–1711.

Lujan, M., Storti, F., Balanya, J.C., Crespo-Blanc, A., Rossetti, F., 2003. Role of decollement material with different rheological properties in the structure of the Aljibe thrust imbricate (Flysch Trough, Gibraltar Arc): an analogue modelling approach. J. Struct. Geol. 25, 867–881.

Mandal, N., Chattopadhyay, A., Bose, S., 1997. Imbricate thrust spacing: experimental and theoretical analyses. In: Sengupta, S. (Ed.), Evolution of Geological Structures in Micro- to Macro-Scales. Chapman and Hall, London, pp. 143–165.

Mitra, G., 1994. Strain variation in thrust sheets across the Sevier fold and thrust belt (Idaho–Utah–Wyoming): implication for section restoration and wedge taper evolution. J. Struct. Geol. 16, 585–602.

Mulugeta, G., 1988. Modeling the geometry of Coulomb thrust wedges. J. Struct. Geol. 10, 847–859.

Mourgues, R., Cobbold, P.R., 2006. Thrust wedges and fluid overpressures: sandbox models involving pore fluids. J. Geophys. Res. 111, B05404, doi:10.1029/2004JB003441.

Mukhopadhyay, D.K., Mishra, P., 2005. A balanced cross section across the Himalayan frontal fold-thrust belt, Subathu area, Himachal Pradesh, India: thrust sequence, structural evolution and shortening. J. Asian Earth Sci. 25, 735–746.

Mukhopadhyay, D.K., Mishra, P., 1999. A balanced cross section across the Himalayan foreland belt, the Punjab and Himachal foothills: a reinterpretation of structural styles and evolution. Proc. Ind. Acad. Sci. Earth Planet. Sci. 108, 189–205.

Mulugeta, G., Koyi, H.A., 1987. Three dimensional geometry and kinematics of experimental piggyback thrusting. Geology 15, 1052–1056.

Mulugeta, G., Koyi, H., 1992. Episodic accretion and strain partitioning in a model sand wedge. Tectonophysics 202, 319–333.

Panian, J., Pilant, W., 1990. A possible explanation for foreland thrust propagation. J. Geophys. Res. 95, 8607–8615.

Persson, K., 2001. Effective indenters and the development of double-vergent orogens: insight from analogue sand models. In: Koyi, H.A., Mancktelow, N. (Eds.), Analogue and Numerical Modelling of Tectonics, Memoir 193. Geological Society of America, pp. 191–206.

Persson, K.S., Sokoutis, D., 2002. Analogue models of orogenic wedges controlled by erosion. Tectonophysics 356, 323–336.

Price, R.A., 1986. The southeastern Canadian Cordillera: thrust faulting, tectonic wedging and delamination of the lithosphere. J. Struct. Geol. 8, 239–254.

Schott, B., Koyi, H.A., 2001. Estimating basal friction in accretionary wedges from the geometry and spacing of frontal faults. Earth Planet. Sci. Lett. 194, 221–227.

Smoluchowski, M.S., 1909. Some remarks on the mechanics of overthrusts. Geol. Mag. 6, 204–205.

Storti, F., McClay, K., 1995. Influence of syntectonic sedimentation thrust wedges in analogue models. Geology 23, 999–1002.

Storti, F., Francesco, S., McClay, K., 2000. Synchronous and velocity-partitioned thrusting and thrust polarity reversal in experimentally produced, doubly-vergent thrust wedges: implications for natural orogens. Tectonics 19 (2), 378–396.

Thakur, V.C., 1993. Geology of Western Himalaya. Phys. Chem. Earth 19, 1–363 (Pergamon Press).

Turcotte, D.L., Schubert, G., 2002. Geodynamics. Cambridge University Press, p. 456.

Willett, S.D., Beaumont, C., 1994. Subduction of Asian lithospheric mantle beneath the Tibet inferred from models of continental collision. Nature 369, 642–645.

Willett, S.D., 1999. Orogeny and orography: the effects of erosion on the structure of mountain belts. J. Geophys. Res. 104, 28957–28981.

Yamada, Y., Baba, K., Matsuoka, T., 2006. Analogue and numerical modeling of accretionary prisms with a decollement in sediments. In: Geological Society of London, Special Publication, vol. 253, pp. 169–183.